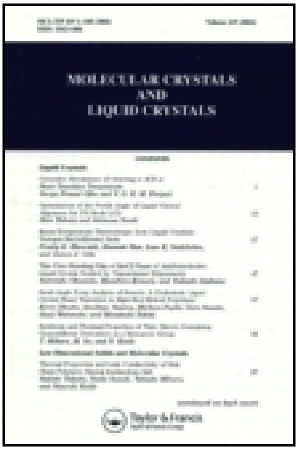

Molecular Crystals and Liquid Crystals

Publication details, including instructions for authors and subscription information:
http://www.tandfonline.com/loi/gmcl20

Synthesis and Physico-Chemical Properties of Polar Liquid Crystal Materials Incorporating a Coumarin Skeleton at the Terminal Position

Yuki Morita [a] , Hiroyuki Ushijima [a] , Kyohei Era [a] , Kazuo Kasatani [a] & Hiroaki Okamoto [a]

[a] Faculty of Engineering, Yamaguchi University, Ube, Yamaguchi, Japan

To cite this article: Yuki Morita, Hiroyuki Ushijima, Kyohei Era, Kazuo Kasatani & Hiroaki Okamoto (2008): Synthesis and Physico-Chemical Properties of Polar Liquid Crystal Materials Incorporating a Coumarin Skeleton at the Terminal Position, Molecular Crystals and Liquid Crystals, 494:1, 282-292

To link to this article: http://dx.doi.org/10.1080/15421400802430000

Mol. Cryst. Liq. Cryst., Vol. 494, pp. 282–292, 2008
Copyright © Taylor & Francis Group, LLC
ISSN: 1542-1406 print/1563-5287 online
DOI: 10.1080/15421400802430000

Synthesis and Physico-Chemical Properties of Polar Liquid Crystal Materials Incorporating a Coumarin Skeleton at the Terminal Position

Yuki Morita, Hiroyuki Ushijima, Kyohei Era, Kazuo Kasatani, and Hiroaki Okamoto
Faculty of Engineering, Yamaguchi University, Ube, Yamaguchi, Japan

*This paper described the synthesis and physico-chemical properties of homologous series of 2-oxo-2*H*-chromen-6-yl 6-alkoxy-naphthalene-2-carboxylate (compounds* **1**-*n). Compounds* **1**-*n show a monotropic nematic (N) phase, where the average of the N-isotropic (I) phase transition temperatures is ca. 140°C. The mesomorphic properties were also examined by binary phase diagrams for the mixture of* **1**-*n ($n = 4$ or 8) and 4-(cyano-4′-octyloxybiphenyl (8 OCB), or 4-heptyloxyphenyl 4-nonyloxybenzoate. The physico-chemical properties for compounds* **1**-*n are compared with the corresponding 4-alkoxybenzoate derivatives (compounds* **2**-*n) and 4-alkoxybiphenyl-4′-carboxylate ones (compounds* **3**-*n). These results are discussed in terms of molecular structures and the electrostatic natures of the molecules.*

Keywords: binary phase diagram; molecular structure; nematic phase; polar liquid crystal; synthesis

INTRODUCTION

It has been known that the mesomorphic and physical properties of liquid crystal materials strongly depend on their molecular structures [1]. It is also well known that the terminal polar groups such as cyano or nitro group, modifying a dielectric anisotropy, have an inevitable role for liquid crystal materials for twisted nematic (TN) mode display devices [2].

This work is supported by Industrial Technology Research Grant Program in 2006 from New Energy and Industrial Technology Development Organization (NEDO) of Japan and Grant-in-Aids for Young Scientists (B) from the Ministry of Education, Culture, Sports, Science and Technology of Japan.

Address correspondence to Hiroaki Okamoto, Department of Advanced Materials Science and Engineering, Faculty of Engineering, Yamaguchi University, Tokiwadai 2557, Ube, Yamaguchi, 755-8611, Japan. E-mail: oka-moto@po.cc.yamaguchi-u.ac.jp

In our earlier papers [3–7], liquid crystal materials having a terminal carbonyl group, such as cyclohexanone, 1,3-dioxa-2-one, benzofuran-2-one, and so on, exhibit a smectic A (SmA) phase with a polar nature. However, these liquid crystal materials are difficult to exhibit a thermally stable nematic (N) phase and are not suitable for applying the TN mode display devices. On the other hand, liquid crystal materials having a 2*H*-pyran-2-one or 2-oxo-2*H*-chromen-6-yl group at the terminal position show a nematic phase [8].

This paper describes that homologous series of 2-oxo-2*H*-chromen-6-yl 6-alkoxy-naphthalene-2-carboxylate (compounds **1**-n) were synthesized and their physico-chemical properties were compared with the corresponding 4-alkoxybenzoate and 4-alkoxybiphenyl-4′-carboxylate derivatives (compounds **2**-n and **3**-n).

Interestingly, compounds **2**-n and **3**-n form organo-gels in various organic solvents [6,9], while compounds **1**-n show no gelation ability, so that mesomorphic properties for compounds **1**-n are reported in this paper (Figure 1).

EXPERIMENTAL

Materials

Compounds **1**-n were synthesized in a moderate yields according to Scheme 1.

The chemical structures were confirmed by ^{1}H NMR and IR spectroscopy, and the purity (99%) was checked by HPLC. The spectra data for compounds **1**-n are shown in appendix.

Method

The transition temperatures and latent heats were determined using a Seiko SSC-5200 DSC, where indium (99.9%) was used as a calibration

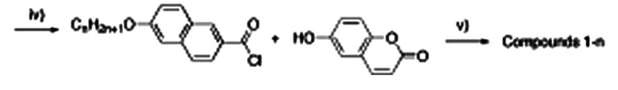

SCHEME 1 Synthetic scheme for compounds **1**-n. Reagents and conditions: i) H_2SO_4, EtOH, reflux for 4 h, 85%; ii) $C_nH_{2n+1}Br$, K_2CO_3, 3-pentanone, reflux for overnight, 52–79%; iii) 6 M NaOH, DMSO, 3 h, then poured into 1 M HCl, 71–93%; iv) $SOCl_2$, 70°C for 1 h; v) Pyridine, toluene, 80°C, overnight, 60–70%.

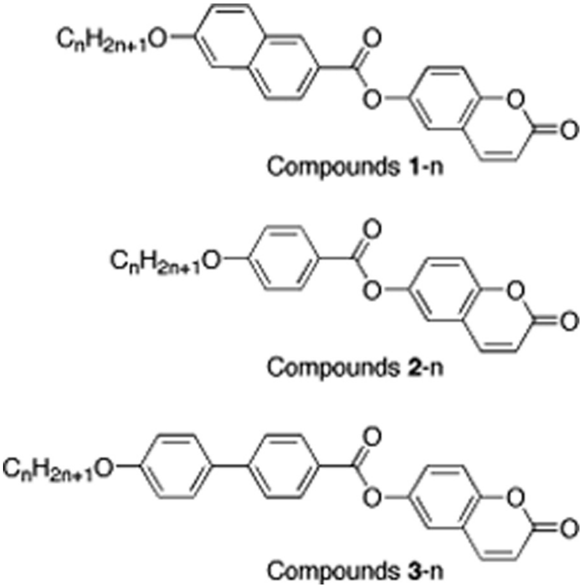

FIGURE 1 Chemical structures for compounds **1**-n–**3**-n

standard (mp = 156.6°C, 28.4 J/g). The DSC thermogram was operated at a heating or cooling rate of 5°C min^{-1}. The mesophases were characterized using a Nikon POH polarizing microscope fitted with a Mettler thermo-control system (FP-900). ^{1}H NMR spectra were measured using a JEOL EX-270 spectrometer, where tetramethylsilane was used as an internal standard. IR spectra were recorded with a Shimadzu Prestige-21 infrared spectrometer. The purity of the materials was checked by HPLC.

TABLE 1 Transition Temperatures (°C) and Latent Heats (kJ mol^{-1}) for Compounds **1**-n

Compounds **1**-n	Transition temperatures (°C)					Latent heats (kJ mol^{-1})	
n	C		N		I	mp	N-I
4	●	168	(●	152)	●	37.3	0.2
5	●	177	(●	140)	●	41.0	0.2
6	●	167	(●	139)	●	38.6	0.4
7	●	159	(●	135)	●	36.9	0.3
8	●	165	(●	137)	●	41.4	0.4

C, N, and I indicate crystal, nematic, and isotropic phases, respectively.
Parentheses indicate a monotropic transition.

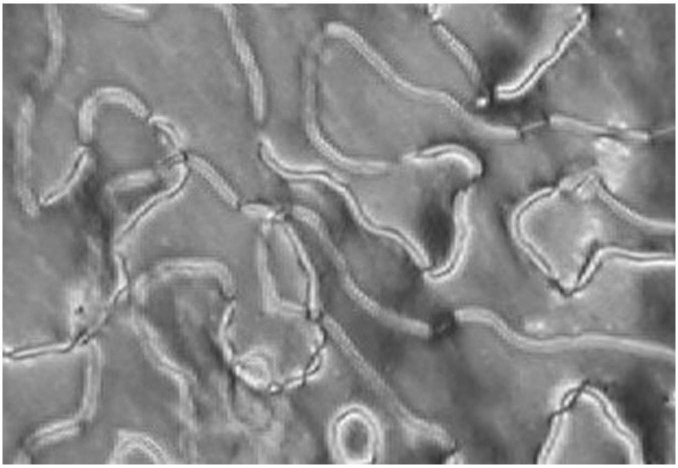

FIGURE 2 Polarized micrograph for compound **1**–5 at 140°C on cooling process.

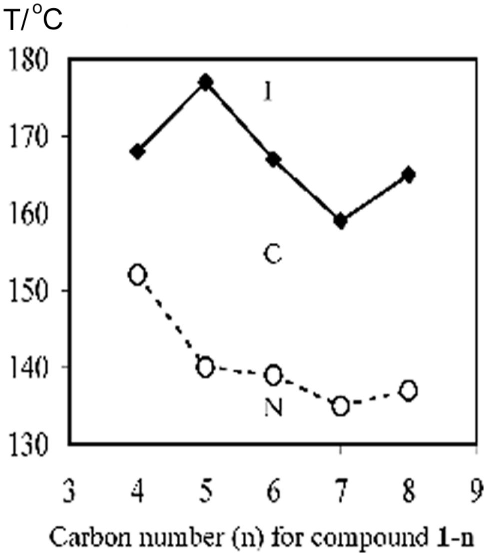

FIGURE 3 Plots of transition temperatures (°C) vs. the carbon number (n) for compounds **1**-n: Diamonds and circles show melting points and nematic–isotropic liquid phase transitions, respectively. Dashed line denotes a monotropic transition.

RESULTS AND DISCUSSION

Thermal properties for compounds **1**-n determined by a differential scanning calorimeter, are summarized in Table 1.

The thermal data for the melting phenomenon were obtained by a first heating process of the crystals obtained by recrystallization from ethanol. The monotropic N-isotropic (I) phase transition data were obtained from a cooling process.

Compound **1**–5, for example, shows an endotherm at 177°C corresponding to melting phenomenon on the first heating process. The molten materials showed a small exotherm at 140°C due to a phase transition on the cooling process.

The formed texture is shown in Figure 2. The mesophase shows a typical schlieren texture at 140°C on cooling process under polarized microscope observation. Therefore, the mesophase for compound **1**–5 is assigned to be a monotropic N phase.

All the homologous series shows a monotropic N phase as shown in Table 1, and the small latent heats for the N-I phase transitions

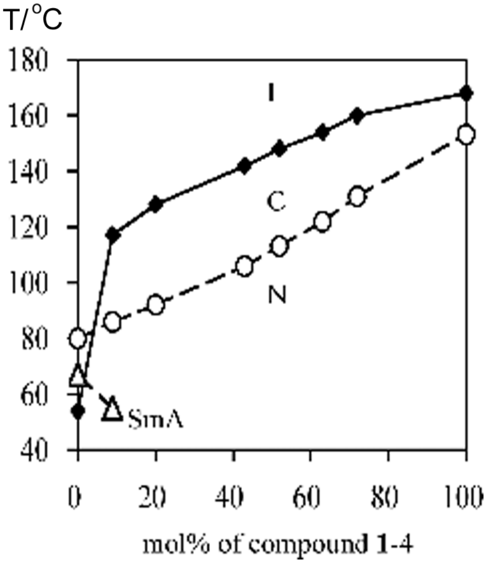

FIGURE 4 Binary phase diagram for the mixture of 4-cyano-4′-octyloxybiphenyl (8OCB) (left) and compound **1**-4 (right): Diamonds, triangles and circles show melting points, smectic A (SmA)–nematic (N) and N–isotropic liquid (I) phase transitions, respectively. Dashed lines denote monotropic transitions.

also agree with the assignment of the N phase. The transition temperatures for compounds **1**-n are plotted against the carbon number (n) as shown in Figure 3.

Compounds **1**-n exhibit an even-odd effect in the N-I transition temperatures and the latent heats. Compounds **2**-n and **3**-n, on the other hand, show the N phase without any even-odd effect, where the average of the N-I transition temperatures are ca. 80°C and 240°C, respectively as described in our earlier papers [8].

Binary phase diagrams for the mixtures of compounds **1** -n (n = 4 or 8) and polar liquid crystal material are examined in order to reveal the mesomorphic property. Figures 4 and 5 show the binary phase diagrams for the mixture of 4-cyano-4′-octyloxybiphenyl (8OCB), a typical polar liquid crystal material, and compounds **1**–4, and **1**–8, respectively. The N phases for compounds **1**–4 and **1**–8 are well miscible with that of 8OCB all over the phase diagrams as shown in Figures 4 and 5.

The N-I transition temperatures increase with increasing the mol concentration of compound **1**–4, while the SmA-N transition temperatures decrease considerably and the SmA phase disappears at 50°C around 10 mol% of compound **1**–4 as shown in Figure 4.

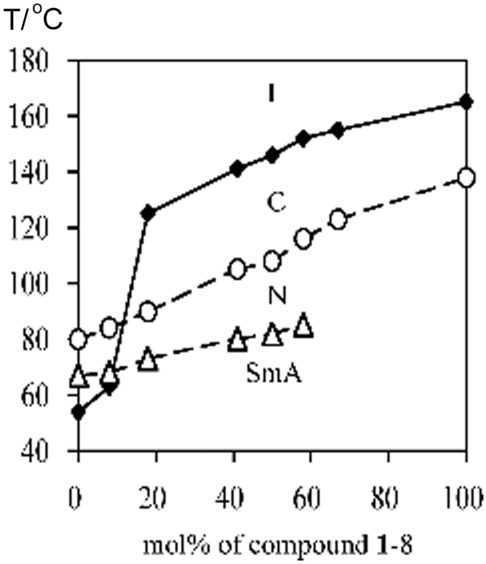

FIGURE 5 Binary phase diagram for the mixture of 8OCB (left) and compound **1**–8 (right): Diamonds, triangles and circles show melting points, SmA-N and N-I phase transitions, respectively. Dashed lines denote monotropic transitions.

Figure 5 shows the binary phase diagram for the mixture of 8OCB and compound **1**–8. The thermal property of the N-I transitions is similar to that in Figure 4, while the SmA-N transition temperatures increase a little with increasing the mol concentration of compound **1**–8. The SmA phase could not observed at ca. 70°C around 60 mol% of **1**–8, because of recrystallization of the mixture. These results indicate the thermal stability of the extrapolated SmA phase is around 100°C, which is extremely lower than that of compound **3**–8 ($T_{SmA\text{-}N} = 208°C$).

Figure 6 shows the binary phase diagram for the mixture of 4-heptyloxyphenyl 4-nonyloxybenzoate and compound **1**–4.

The transition temperatures of the smectic phase considerably increase with increasing the mol concentration of compound **1**–4, in spite of showing no smectic property. The SmA-I transition temperatures show a notable upward convexity around 40 mol% of compound **1**–4, and then the SmA phase disappears around 70 mol%.

A similar tendency is also observed in the phase diagram for the mixture of 4-heptyloxyphenyl 4-nonyloxybenzoate and compounds

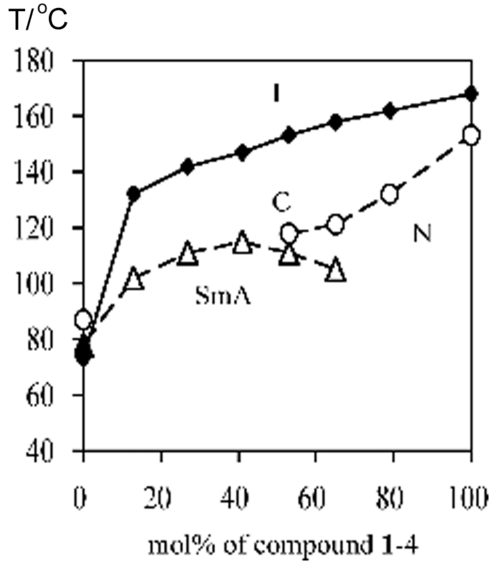

FIGURE 6 Binary phase diagram for the mixture of 4-heptyloxyphenyl 4-nonyloxybenzoate (left) and compound **1**–4 (right): Diamonds, triangle (filled) triangles (open) and circles show melting points, SmC-N, SmA-N and N-I phase transitions, respectively. Dashed lines denote monotropic transitions.

1–8 as shown in Figure 7, where the maximum SmA-N transition temperature is 120°C around 70 mol% of **1**–8.

It is well known that a lot of liquid crystal mixtures consisting of polar and non-polar liquid crystals show a notable enhancement and/or an induction of the SmA phase. In these phenomena, dipole–dipole and/or electron donor–acceptor interactions are considered to play important roles [10]. In Figures 6 and 7, the polar and non-polar components correspond to compounds **1**-n and 4-heptyloxyphenyl 4-nonyloxybenzoate, respectively.

These results indicate that the terminal coumarin skeleton for compounds **1**-n gives a polarity in the liquid crystal core.

The molecular structures and dipole moments for compounds **1**–8, **2**–8 and **3**–8 are calculated by a semi-empirical molecular orbital calculation (MOPAC, AM1) [11], and the molecular dimensions and dipole moments are shown in Figure 8.

The calculated dipole moments for compounds **1**–8, **2**–8 and **3**–8 are similar (8 D), while the molecular lengths are different due to the core structures. Interestingly, the molecular breadths are almost the same and independent of the core structures. Therefore, the order

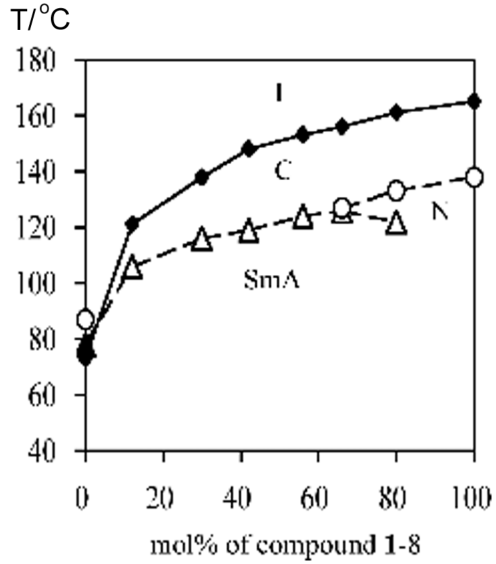

FIGURE 7 Binary phase diagram for the mixture of 4-heptyloxyphenyl 4-nonyloxybenzoate (left) and compound **1**–8 (right): Diamonds, triangle (filled) triangles (open) and circles show melting points, SmC-N, SmA-N and N-I phase transitions, respectively. Dashed lines denote monotropic transitions.

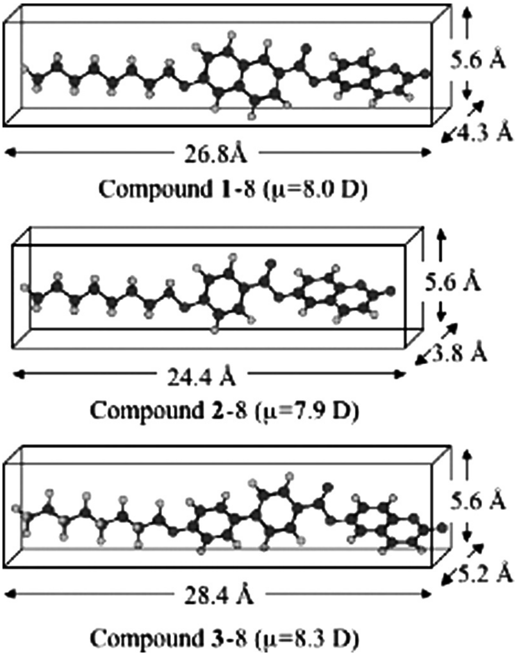

FIGURE 8 Molecular structures, dimensions and dipole moments for compounds **1**–8, **2**–8, and **3**–8, calculated by a semi-empirical molecular orbital calculation (MOPAC, AM1) [11].

of the length-to-breadth ration is as follows; **3**-8 (5.07) > **1**–8 (4.79) > **2**–8 (4.36), and similar to the order of the N-I phase transition temperatures.

It is well known that the length-to-breadth ratio also causes the even-odd alternation on the N-I phase transition temperatures [12]. Only compounds **1**-n show the even-odd alternation as described before, indicating that the core structure also affects the even-odd effect on the N-I phase transition temperatures.

CONCLUSION

We have prepared a homologous series of compounds **1**-n, which show the monotropic N phase with the even-odd effect on the N-I phase transition temperatures and latent heats. The N-I transition temperature for compound **1**–8 is ca. 140°C. The terminal coumarin skeleton gives a polarity in the liquid crystal core.

REFERENCES

[1] Gray, G. W. (1972). *Advances in Liquid Crystals*, Academic Press Inc.: New York and London, Vol. 2.

[2] Pohl, L. & Finkenzeller, U. (1990). Physical properties of liquid crystals. In: *Liquid Crystals, Application and Uses*, Bahadur B., (Ed.), World Scientific: Singapore, Ch. 4, Vol. 1, p. 140.

[3] Okamoto, H., Okamoto, T., & Takenaka, S. *Chem. Lett.*, *2000*, 1040.

[4] Okamoto, H., Okamoto, T., Petrov, V. F., & Takenaka, S. (2001). *Mol. Cryst. Liq. Cryst.*, *364*, 719.

[5] Morita, Y., Tasaka, T., Habu, K., Okamoto, H., Kasatani, K., & Takenaka, S. (2004). *Trans. Mater. Res. Soc. Jpn.*, *29*, 831.

[6] Zhang, F., Morita, Y., Kawabe, K., Tasaka, T., Okamoto, H., & Takenaka, S. (2005). *Chem. Lett.*, *34*, 1156.

[7] Morita, Y., Zhang, F., Tasaka, T., Yamaguchi, R., Okamoto, H., & Takenaka, S. (2006). *Bull. Chem. Soc. Jpn.*, *79*, 163.

[8] Morita, Y., Tasaka, T., Yamaguchi, R., Okamoto, H., & Takenaka, S. (2005). *Mol. Cryst. Liq. Cryst.*, *439*, 2075.

[9] Morita, Y., Kawabe, K., Zhang, F., Okamoto, H., Takenaka, S., & Kita, H. (2005). *Chem. Lett.*, *34*, 1650.

[10] Kelker, H. & Hatz, R. (1980). *Handbook of Liquid Crystals*, Verlag Chemie: Weinheim, 340.

[11] Dewar, M. J. S., Zoebisch, E. G., Healy, E. F., & Steward, J. J. P. (1985). *J. Am. Chem. Soc.*, *107*, 3902.

[12] Demus, D. (1998). Chemical structure and mesogenic properties. In: *Handbook of Liquid Crystals*, Demus, D., Gooby, J., Gray, G. W., & Spiess, H.-W., (Eds.), Wiley-VCH: Weinheim, Chapter 6, Vol. 1.

APPENDIX

Spectra data for compounds **1**-n are as follows:

Compound **1**–4; IR (KBr disc) $\nu = 1190.0$, 1718.5, 1741.7, and 2941.4 cm^{-1}, ^{1}H NMR (CDCl$_3$) $\delta = 1.02$ (3H, t, $J = 7.3$ Hz), 1.57 (2H, six., $J = 7.6$ Hz), 1.86 (2H, qui., $J = 6.7$ Hz), 4.13 (2H, t, $J = 6.6$ Hz), 6.48 (1H, d, $J = 9.6$ Hz), 7.19 (1H, d, $J = 2.3$ Hz), 7.23 (1H, dd, $J = 8.9$, 2.3 Hz), 7.38–7.48 (3H, m), 7.70 (1H, d, $J = 9.8$ Hz), 7.81 (1H, d, $J = 8.6$ Hz), 7.88 (1H, d, $J = 8.9$ Hz), 8.13 (1H, dd, $J = 8.6$, 1.7 Hz), 8.69 (1H, d, $J = 1.3$ Hz) ppm.

Compound **1**–5; IR (KBr disc) $\nu = 1190.0$, 1718.5, 1741.7, and 2926.0 cm^{-1}, ^{1}H NMR (CDCl$_3$) $\delta = 0.96$ (3H, t, $J = 7.0$ Hz), 1.38–1.56 (4H, m), 1.87 (2H, qui., $J = 6.6$ Hz), 4,12 (2H, t, $J = 6.3$ Hz), 6.48 (1H, d, $J = 9.6$ Hz), 7.18 (1H, d, $J = 2.4$ Hz), 7.22 (1H, dd, $J = 8.9$, 2.2 Hz), 7.38–7.44 (3H, m), 7.70 (1H, d, $J = 9.6$ Hz), 7.81 (1H, d, $J = 8.9$ Hz), 7.88 (1H, d, $J = 8.9$ Hz), 8.13 (1H, dd, $J = 9.0$, 1.9 Hz), 8.69 (1H, d, $J = 1.4$ Hz) ppm.

Compound **1**–6; IR (KBr disc) $\nu = 1190.1$, 1718.5, 1741.7, and 2926.0 cm^{-1}, ^{1}H NMR (CDCl$_3$) $\delta = 0.93$ (3H, t, $J = 7.4$ Hz), 1.37–1.57

(6H, m), 1.87 (2H, qui., $J = 6.6\,\text{Hz}$), 4, 12 (2H, t, $J = 6.3\,\text{Hz}$), 6.48 (1H, d, $J = 9.5\,\text{Hz}$), 7.18 (1H, d, $J = 2.3\,\text{Hz}$), 7.23 (1H, dd, $J = 8.3, 2.3\,\text{Hz}$), 7.38–7.46 (3H, m), 7.70 (1H, d, $J = 9.6\,\text{Hz}$), 7.81 (1H, d, $J = 8.6\,\text{Hz}$), 7.88 (1H, d, $J = 8.9\,\text{Hz}$), 8.13 (1H, dd, $J = 8.6, 1.6\,\text{Hz}$), 8.69 (1H, d, $J = 1.3\,\text{Hz}$) ppm.

Compound **1**–7; IR (KBr disc) $\nu = 1192.0$, 1712.7, 1741.7, and $2922.1\,\text{cm}^{-1}$, ^{1}H NMR ($CDCl_3$) $\delta = 0.91$ (3H, t, $J = 7.1\,\text{Hz}$), 1.26–1.57 (8H, m), 1.88 (2H, qui., $J = 6.6\,\text{Hz}$), 4,12 (2H, t, $J = 6.6\,\text{Hz}$), 6.48 (1H, d, $J = 9.5\,\text{Hz}$), 7.18 (1H, d, $J = 2.0\,\text{Hz}$), 7.24 (1H, dd, $J = 8.9, 2.4\,\text{Hz}$), 7.36–7.45 (3H, m), 7.70 (1H, d, $J = 9.6\,\text{Hz}$), 7.81 (1H, d, $J = 8.6\,\text{Hz}$), 7.88 (1H, d, $J = 8.9\,\text{Hz}$), 8.13 (1H, dd, $J = 8.6, 1.7\,\text{Hz}$), 8.69 (1H, d, $J = 1.3\,\text{Hz}$) ppm.

Compound **1**–8; IR (KBr disc) $\nu = 1192.0$, 1716.6, 1741.7, and $2922.1\,\text{cm}^{-1}$, ^{1}H NMR ($CDCl_3$) $\delta = 0.90$ (3H, t, $J = 6.3\,\text{Hz}$), 1.24–1.59 (10H, m), 1.87 (2H, qui., $J = 6.6\,\text{Hz}$), 4,12 (2H, t, $J = 6.6\,\text{Hz}$), 6.48 (1H, d, $J = 9.6\,\text{Hz}$), 7.18 (1H,d, $J = 2.3\,\text{Hz}$), 7.24 (1H, dd, $J = 8.9, 2.3\,\text{Hz}$), 7.38–7.45 (3H, m), 7.70 (1H, d, $J = 9.5\,\text{Hz}$), 7.81 (1H, d, $J = 8.6\,\text{Hz}$), 7.88 (1H, d, $J = 9.2\,\text{Hz}$), 8.13 (1H, dd, $J = 8.6, 2.0\,\text{Hz}$), 8.69 (1H, d, $J = 1.3\,\text{Hz}$) ppm.